CHAPTER 2 Principle and Design

The binary and gray-scale microlens will be designed and fabricated. Silicon nitride and photoresist will be taken as the material of the microlens in this thesis. The design of the microlens is based on the material properties of the photoresist and silicon nitride, formula of microlens, and Focus Ion Beam (FIB) characteristics. In this chapter, the design of microlenses is discussed.

2-1 Material property

2-1-1 Photoresist AZ4620

A photoresist is a polyethylene macromolecular compound that comprises three basic constituents: a base resin, a photoactive inhibitor, and a solvent. The resin is used as a kind of binder. The photoactive inhibitor literally is a material with properties can be changed by light source. And the concentration of photoactive inhibitor strongly influences the dissolution rate of the photoresist in a developer solution. The solvent is used to render a mixture of photoresist resin and photoactive inhibitor into a liquid form. This allows for spin coating of the resulting photoresist onto a wafer.

Photoresist can be modeled based on photoresist linearization [17]. In order to develop the model of photoresist, it is assumed that the photoresist can only be divided into two parts, material C that do not expose to UV irradiation and material S that changed after UV irradiation. For a positive photoresist, the development rate of material C is denoted D_C, and the development rate of material S, Ds, and $D_S >> D_C$. In the following derivation, the percentage of material C is denoted as C, and the percentage of material S as S. Now consider a positive photoresist for which initially

at $t=0$ the film is entirely unexposed:

$$S_{t=0} = S(0) = 0,$$

$$C_{t=0} = C(0) = 1. \tag{2-1}$$

The film is then transformed during an exposure interval Δt. Assume that the change ΔS is proportional to the amount of unchanged material C and to the intensity I of UV light, according to

$$\Delta S(t) = \mu C(t) I \Delta t. \tag{2-2}$$

The constant μ is the optical response parameter, which describes the material's sensitivity to UV irradiation. And the total amount of photoresist is conserved during the process:

$$S(t) + C(t) = 1. \tag{2-3}$$

Thus solving Equation (2-2) and (2-3) and enforcing the initial condition in Equation (2-1), one can obtain

$$S(t) = 1 - \exp(-\mu I t). \tag{2-4}$$

In the gray-scale technique the intensity is controlled by the mask, which has a transmittance T. The intensity of light that reaches the photoresist is $I = I_0 T$, where I_0 is the intensity without the mask. After t_0 seconds of exposure the percentage of material S is

$$S(t) = 1 - \exp(-\mu I_0 T t_0). \tag{2-5}$$

Then define a variable $\kappa = \mu I_0 t_0$, equation (2-5) becomes

$$S(t) = 1 - \exp(-\kappa T). \tag{2-6}$$

The depth of the developed photoresist is proportional to the solubility of the final material, which is also proportional to S:

$$\text{Solubility} = D_S S + D_C (1 - S) = D_C + (D_S - D_C)S \tag{2-7}$$

From Equation (2-5), the percentage of chemical change in the resist is not directly linear to the transmittance. The relation can be seen more clearly in Figure 2-1.
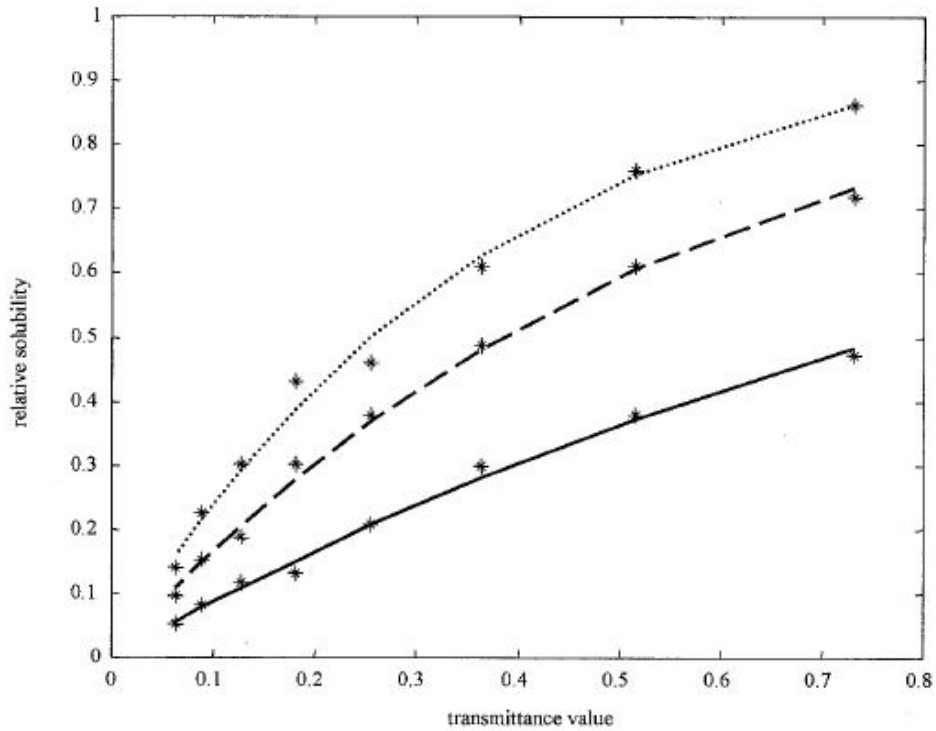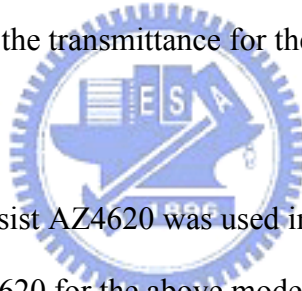
Figure 2-1: Solubility versus the transmittance for the photoresist samples [17].

In this thesis, the photoresist AZ4620 was used in the grayscale photolithography. To find the parameters of AZ4620 for the above model, the resist was spin coated with the recipe of spread cycle = 1000rpm for 10 seconds and spin cycle speed = 2750rpm for 35 seconds. The obtained resist thickness was 8μm. The resist was exposed through a pattern consisting of areas with transmittance from 0.017 to 0.232. The energy of the UV light of the lithography system was measured and the exposure time was fixed to 90 seconds. Next, the development time was adjusted to obtain as many gray levels in the resist as possible. Then different depths of the developed photoresist were measured. Finally, the relative solubility versus transmittance was obtained and shown as Figure 2-2.
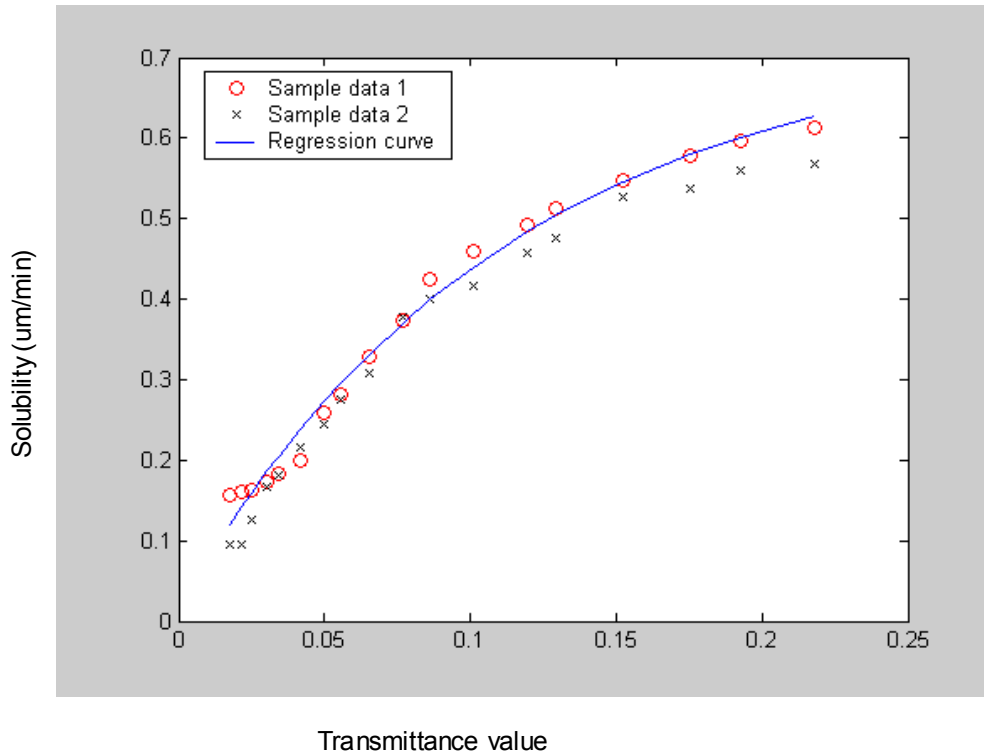
Transmittance value

Figure 2-2: Solubility versus the transmittance for AZ4620.

In Figure 2-2, the parameters for the model of photoresist linearization are: the solubility of the material S, $D_S = 0.6893 \mu m / \min$, the solubility of the material C, $D_C = 0.0003 \mu m / \min$, and the optical response parameter, $\mu = 0.015$. The relation $D_S \gg D_C$ is reasonable for the positive photoresist AZ4620. The model established in the Figure 2-2 will be used to design the gray-scale mask of FIB method.
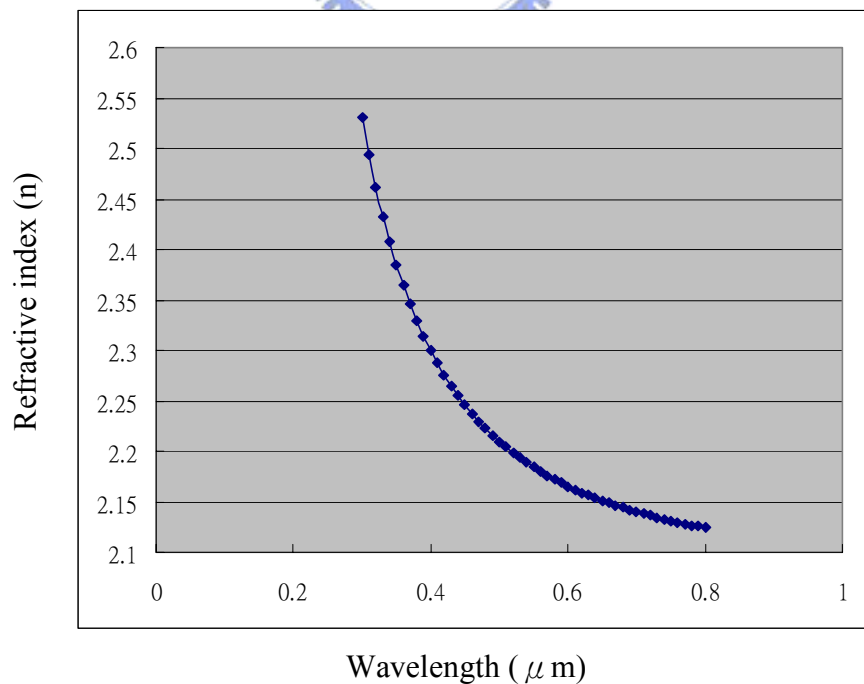
2-1-2 Silicon Nitride

Silicon nitride is a commonly used material in microcircuit and microsensor fabrication due to its many superior chemical, electrical, optical, and mechanical properties [18]. Some applications of silicon nitride are optical waveguides (nitride/oxide), insulators, mechanical protection layer, etch mask, oxidation barrier, and ion implant mask. Silicon nitride is also hard, with a Young's modulus higher than that of Si, and it can be used, for example, as a bearing material in micromotors.

21

Silicon nitride can be deposited by a wide variety of CVD techniques (LPCVD and PECVD). Nitride often deposited from SiH_4 or other Si containing gases and NH_3 in a reaction such as:

$$3SiCl_2H_2+4NH_3 \rightarrow Si_3N_4+6HCl+6H_2$$
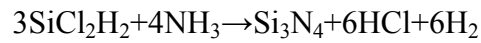
In the IC industry, silicon nitride is LPCVD deposited at 700 to 900°C and at 200 to 500mTorr and functions as an oxidation mask and as a gate dielectric in combination with thermally grown SiO_2. In micromachining, LPCVD nitride serves as an important mechanical membrane material and isolation/buffer layer.

The optical property measurement of silicon nitride, refractive index n and extinction coefficient k by LPCVD process is shown in Figure 2-3. However, absorption increases sharply in the violetblue region, and it can be noticed that the low-stress silicon nitride is characterized by the strongest absorption in this short-wavelength range, so that it can be used as a mask.
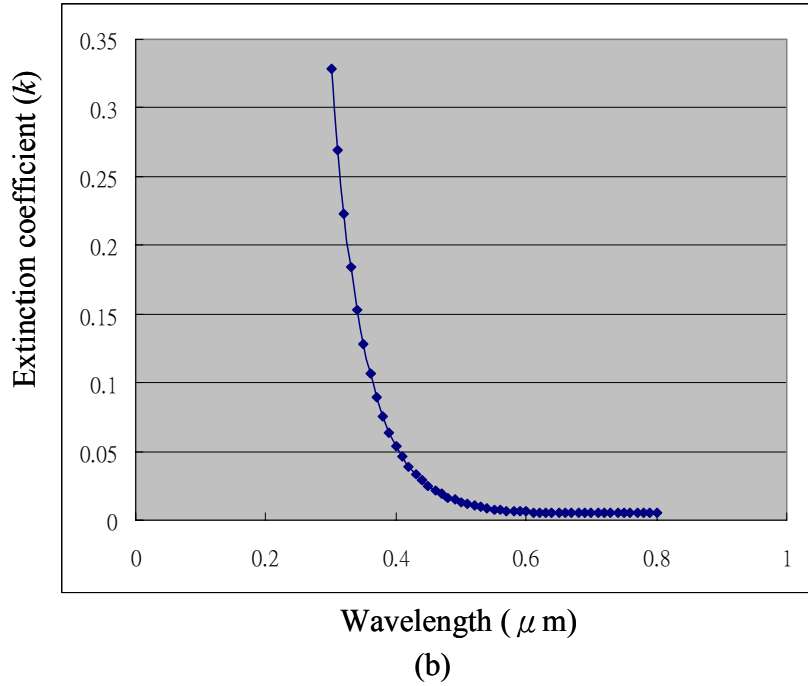

(a)

Wavelength (μm)

(b)

Figure 2-3: (a) Refractive index of LPCVD silicon nitride, (b) extinction coefficient.

2-2 Lens design

In mircooptics, a diffractive type microlens plays an important role. This is due to the large functionality of computer-designed diffractive elements that can be used to fabricate unusual individual elements. In this paper, the Lensmaker's Formula was used:

$$\frac{1}{f} = (n-1)(\frac{1}{r_1} + \frac{1}{r_2}),$$ (2-8)

where f is the focal length, n is the index of refraction of the microlens relative to the air, r_1 and r_2 are the radius of each side of the microlens. More precisely, the Lensmaker's Formula has been revised to a more accurate one [19], as shown in Figure 2-4:

$$\frac{1}{f} = (n-1)(\frac{1}{r_1} - \frac{1}{r_2} + \frac{(n-1)T_C}{nr_1r_2}),$$ (2-9)

$$P_1 = -\frac{f(n-1)T_C}{nr_2},$$ (2-10)

$$P_2 = -\frac{f(n-1)T_C}{nr_1},\qquad\qquad\qquad (2\text{-}11)$$

where T_C is the thickness of the microlens, P_1 is the distance of the primary

principal plane, H_1, to the vertex of the lens, V_1, P_2 is the distance of the secondary

principal plane, H_2, to the vertex of the lens, V_2. In this paper, the positive

photoresist AZ4620 has a refractive index n of 1.62, and the radiuses of the microlens,

r_1 and r_2 are $50\,\mu m$ and ∞, respectively. Because r_2 is infinity, P_1 will be zero.

For the requirement of the DVD micro pick-up head, the numerical aperture (NA)

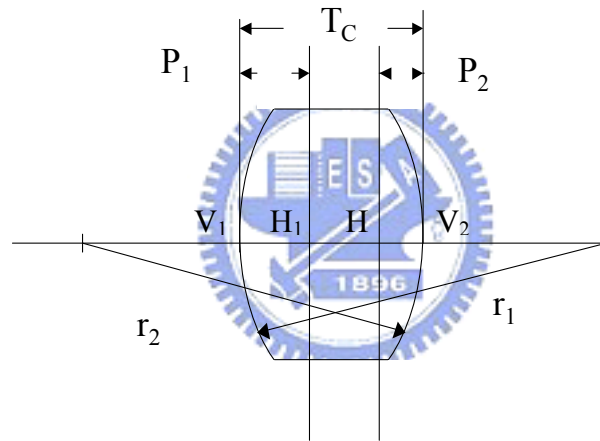shown in Figure 2-5 has been fixed to 0.65.

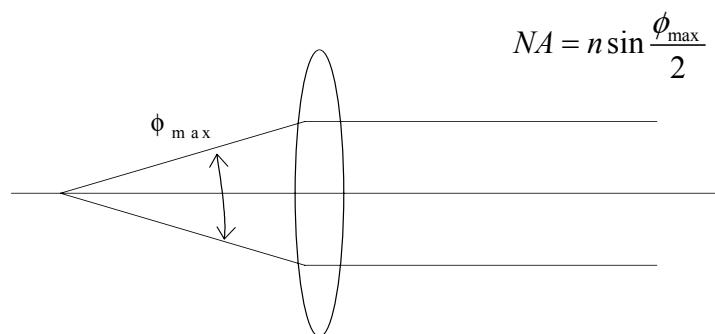Figure 2-4: Diagram for the Lensmaker's Formula.

Figure 2-5: Diagram of the numerical aperture.

According to the Equations, (2-9), (2-10), and (2-11), the lens can be designed, as listed in Table 2-1. Herein, two radiuses have been used due to the restriction of FIB system. In Table 2-1, the thickness of the microlens is too large, so Equation (2-12) will be used to cut the thickness of the microlens, as described in Chapter 1.

$$h = \frac{\lambda}{n-1} \times m, \qquad (2\text{-}12)$$

where h is the cut thickness, λ is the wave length of the incident light, and m is an integer. When the cut thickness is small, the minimum width will be too small for the lithography system. However, when the cut thickness is large, the thickness of the microlens will too large for fabrication. So by the calculation with m chosen as 3, the cut thickness, h is $3.073\,\mu m$. The calculated profiles of the microlens are shown in Figures 2-6 and 2-7, and the calculated values are shown in Table 2-2, where the maximum thickness is h, minimum thickness is the thickness of the middle circle, maximum width is the radius of the middle circle, and minimum width is the width of the outmost ring.
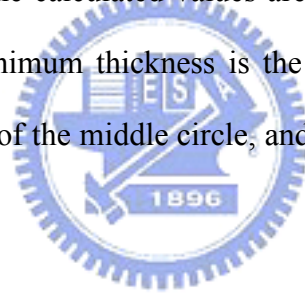
Table 2-1: Calculation of the lens design

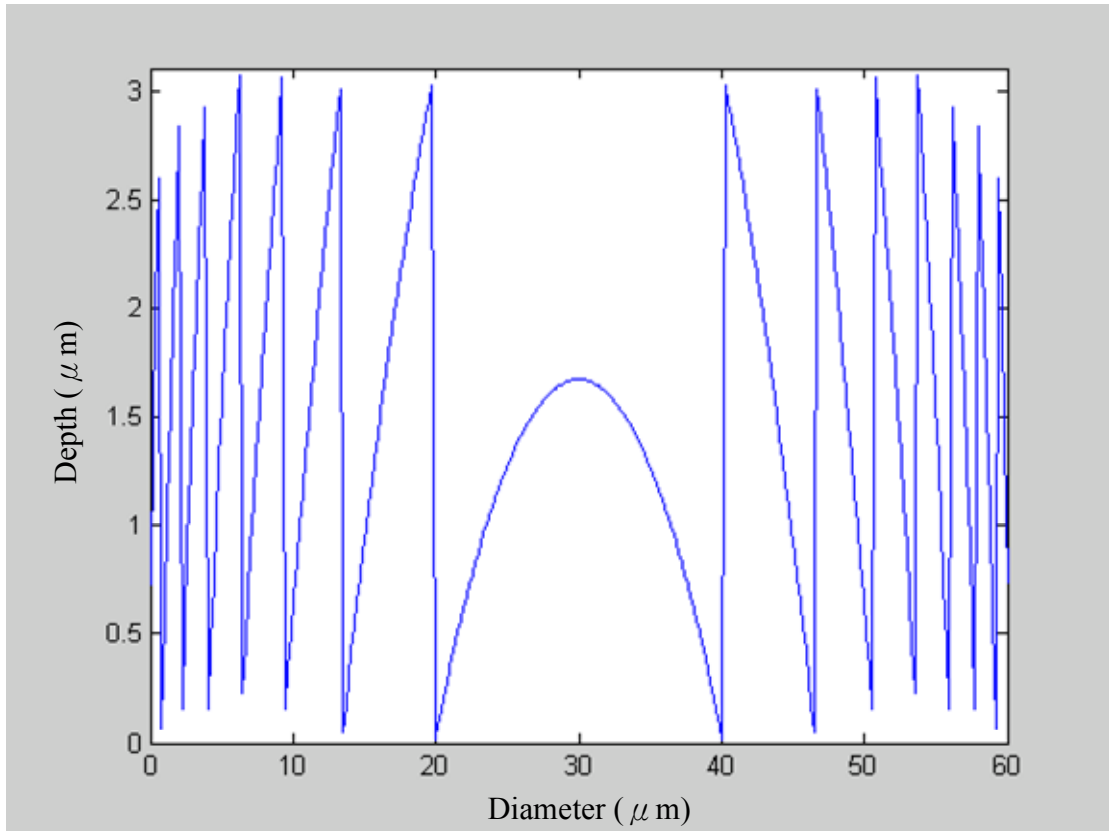| Initial condition		Calculated value			
n	r (μm)	f (μm)	aperture (μm)	thickness (μm)	NA
1.6176	31	50.19	60	23.19	0.65
1.6176	52	84.20	100	37.72	0.65

Figure 2-6: Design of the microlens (aperture :60 μ m).
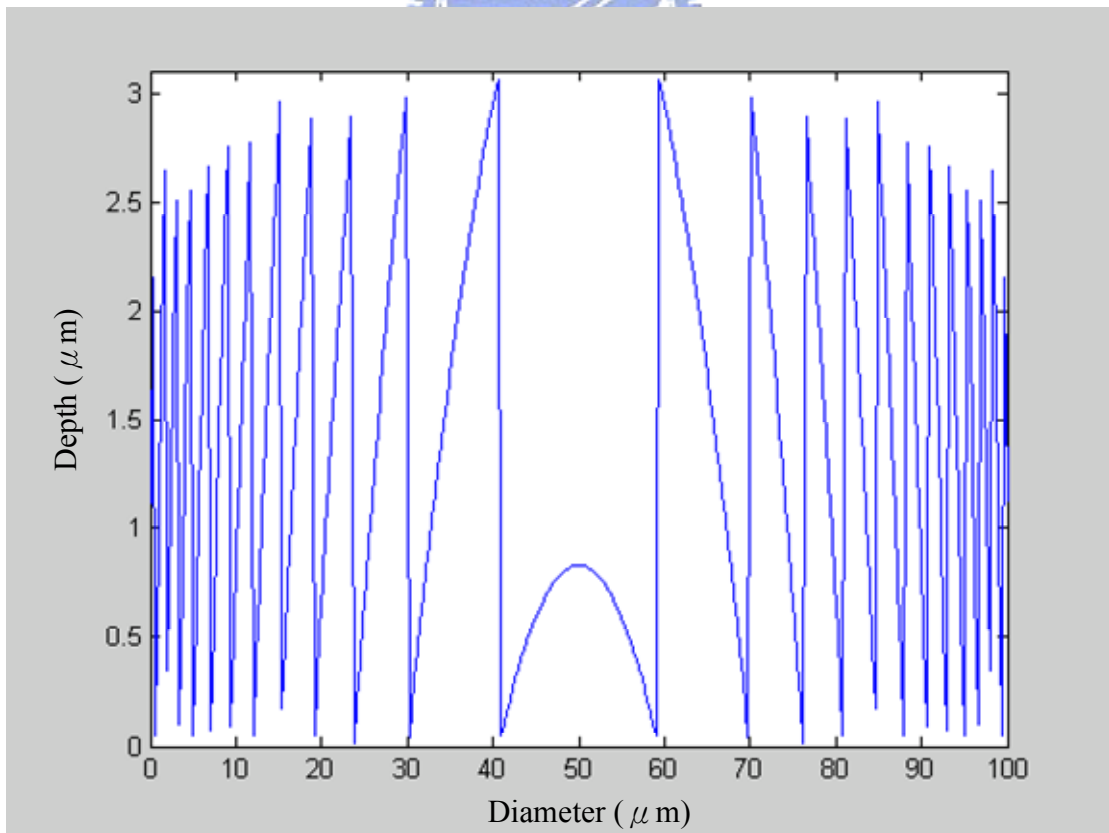

Figure 2-7: Design of the microlens (aperture : 100 μ m).

Table 2-2: Calculated values of sliced microlens.

Aperture	Maximum thickness	Minimum thickness	Maximum width	Minimum width
60 μm	3.073 μm	1.67 μm	20.08 μm	0.97 μm
100 μm	3.073 μm	0.83 μm	21.02 μm	0.98 μm

2-3 Binary design

A diffractive microlens is a micro-optical component as small as a few tens of microns in diameter and with a thickness on the order of an optical wavelength. A binary diffractive microlens is an approximation of a kinoform, or continuous diffractive lens, designed by applying a phase-function constraint between 0 and 2π to subtract an integral number of wavelengths from the lens transmittance function. Theoretically, a kinoform lens has a 100% diffraction efficiency. Multilevel lithography and stepwise etching can approximate the kinoform lens structure.
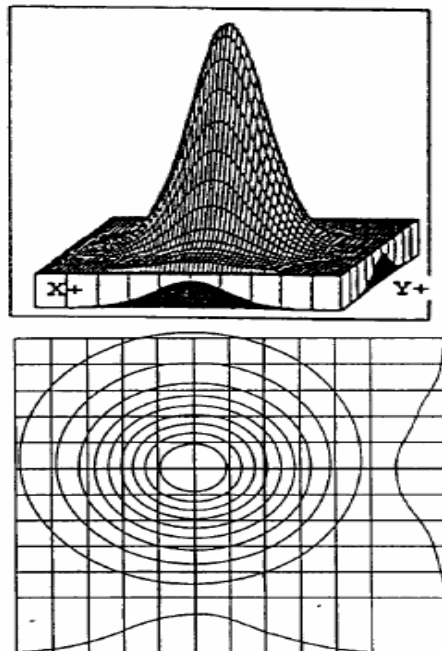

Figure 2-8: Intensity profile and contour plot of an optical beam collimated by a binary micro-Fresnel lens [20].

The binary lens also can exhibits good optical performance. Figure 2-8 is an intensity profile and contour plot of the optical beam emitted from an optical fiber and collimated by the two-phase binary micro-Fresnel lens [20]. Good agreement with a Gaussian shape was obtained. The intensity full-width-at-half-maximum (FWHM) divergence angle of the collimated beam has been reduced from 5.0° to 0.33°. The diffraction efficiency of this two-phase micro-Fresnel lens was measured to be 8.6% [21]. This is in agreement with the theoretical limit of the binary Fresnel zone plate.

Multilevel Fresnel lenses at the expense of more complicated fabrication processes can achieve an efficiency greater than 80%. Figure 2-9 shows a processing cycle for fabrication of a binary-optics microlens. Figure 2-9(a), 2-9(b), and 2-9(c) illustrate the process of a two-phase, four-phase, and eight-phase microlens.

(a)

TWO PHASE-LEVEL STRUCTURE

(b)

FOUR PHASE-LEVEL STRUCTURE
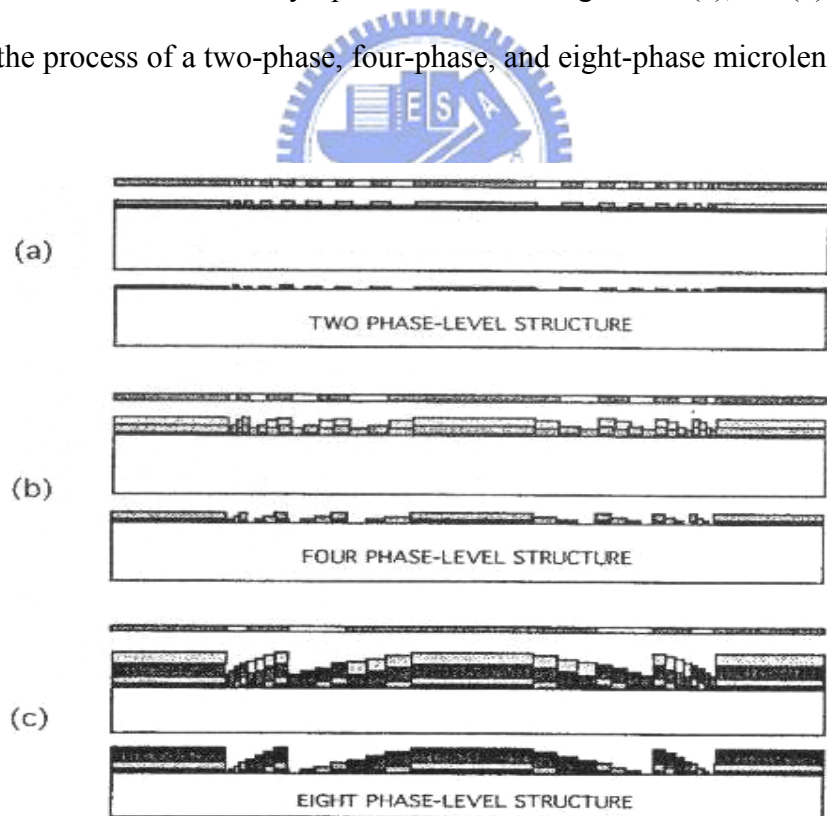
(c)

EIGHT PHASE-LEVEL STRUCTURE

Figure 2-9: Processing cycles of multi-level binary-optics microlens

For a multilevel binary optical structure, the etch depth of each level is defined by the relation [22]

$$d(m) = \frac{\lambda}{(n-1)2^m}, \tag{2-13}$$

where λ is the light wavelength in free space, n is the index of refraction of the lens material, m is the mask number for the level-m process, and $d(m)$ is the etch depth of the level m. An m-mask process produces an $M=2^m$ step approximation to a continuous diffractive structure.

Since microlenses operate over a small range in incident angle, a simple planar thin-film lens design is acceptable. The optical path difference (OPD) function for each lens is used to derive the following relationship among the zone radius, focal length, and wavelength [22]:

$$r(p,m) = [(\frac{p\lambda}{n2^m})^2 + 2f(\frac{p\lambda}{n2^m})]^{1/2}, \tag{2-14}$$

where f is the focal length, p=0, 1, 2, 3… is the ring number, n is the index of refraction of the substrate, and $r(p, m)$ gives the successive zone radii for the patterns in mask number m.

In this study, the four-phase binary Fresnel lens is used. The odd annular rings are used in the mask design of this thesis. The following is the width of each ring of a $485\,\mu m$ focal length lens calculated from Equation (2-14). The diameter of the first circle is $13.8\,\mu m$. The widths of the other layout rings in turn are $4.4\,\mu m$, $3.3\,\mu m$, $2.7\,\mu m$, $2.4\,\mu m$, $2.1\,\mu m$, and $2\,\mu m$. Figure 2-10(a) is the layout of $485\,\mu m$ focal length of Fresnel lens in accordance with those calculated values. In this layout, the four bars support and link the rings.
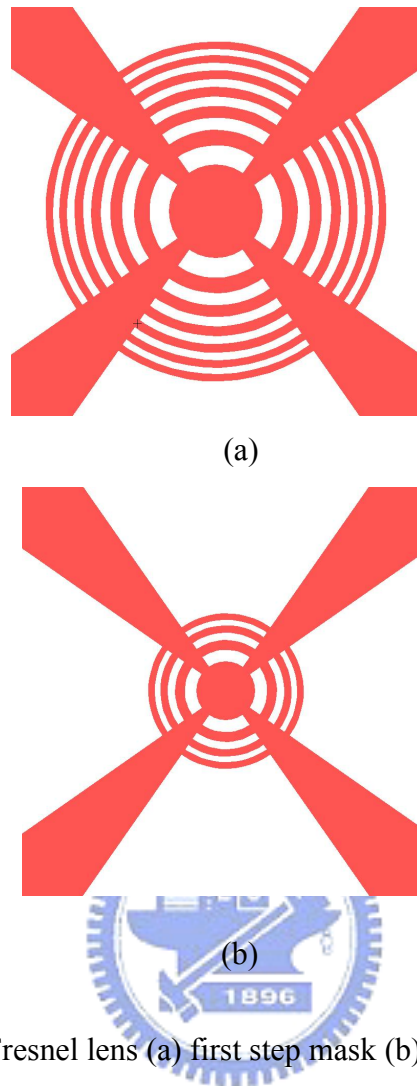
(a)

(b)

Figure 2-10: Fresnel lens (a) first step mask (b) second step mask.

Figure 2-10(b) is the layout of second step mask in accordance with the calculated values. The following is the width of each ring of second step mask calculated from Equation (2-10). The diameter of the first circle is 9.8μm. The widths of the other layout rings in turn are 3.1 μm , 2.3 μm , and 2 μm . The minimum width of these two masks is limited by constrain of the laser pattern generator to 2 μm .

2-4 FIB mask design

The FIB system has been discussed in Chapter 1, and the milling application is used to fabricate gray-scale mask. In this thesis, the FIB system was used to define the pattern on the mask. According to the photoresist model in Figure 2-2, the

transmittance of the silicon nitride mask, and lens design, and the FIB profile can be determined. In the first step, the pixel number in the designed pattern should be set. For a good approximation, the pixelss should be as many as possible. However, the FIB system has a constraint of the maximum number of pixels. After testing four pixel matrix, 50×50, 100×100, 200×200, and 300×300, the last one can be achieved. So the 300×300 pixel matrix is chosen. Then the two-dimensional pattern of the microlens should be sampled by the pixel matrix. Next, the two-dimensional pattern was transferred to a three-dimensional structure. And the FIB gray-scale pattern is shown in Figure 2-11 and 2-12.
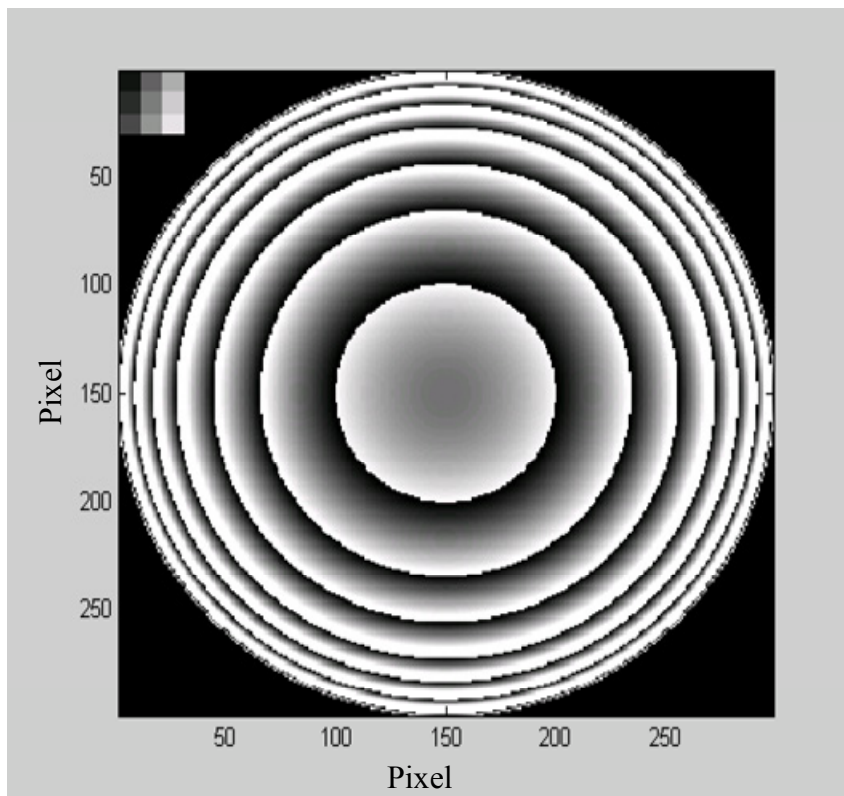

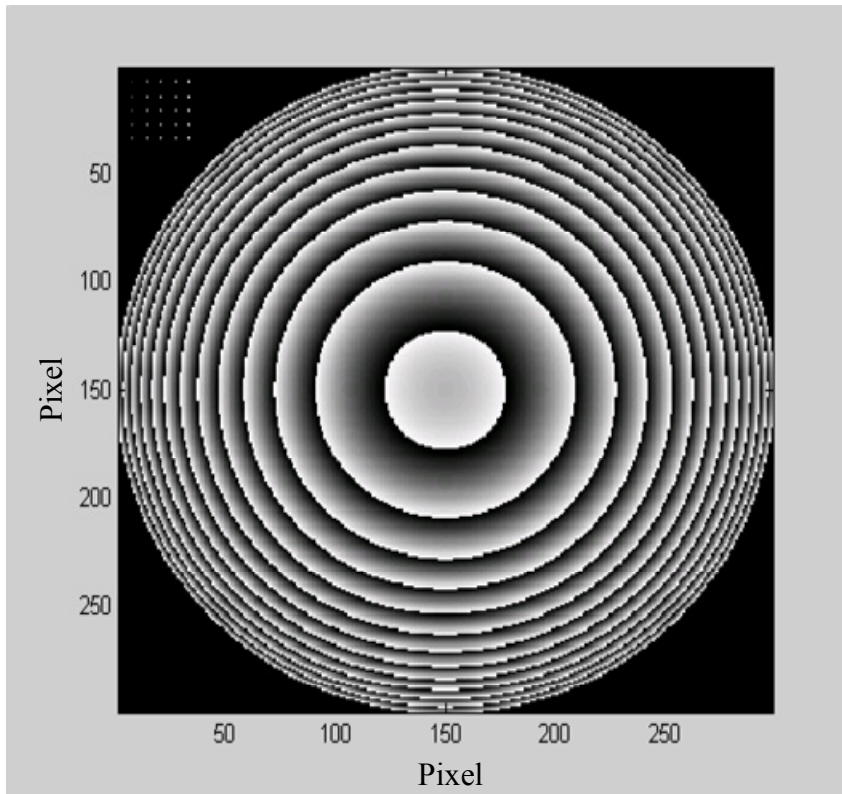Figure 2-11: Gray-scale of the FIB design pattern (aperture=60 μ m)

Figure 2-12: Gray-scale of the FIB design pattern (aperture=100 μ m)

CHAPTER 3 Fabrication

The mask and microlens fabrication process are discussed in this chapter.

3-1 Binary microlens process

The binary mask process is discussed in Sec. 2-3, and the negative photoresist SU-8 is taken as the material of diffractive microlens. The process is shown in Figure 3-1.

Substrate (Si)
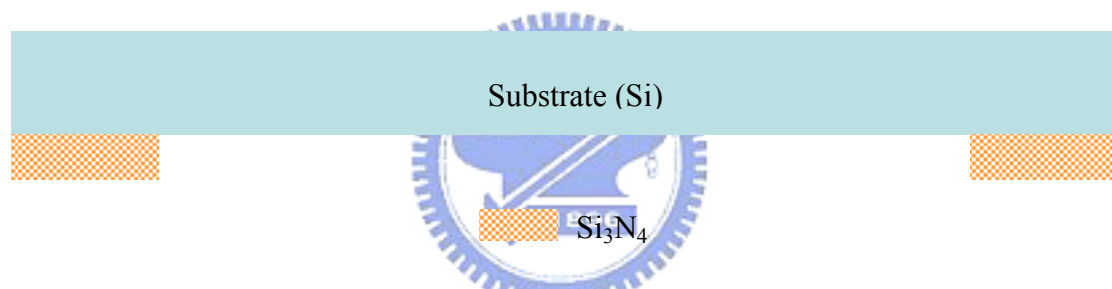
Si_3N_4

1. Deposit silicon nitride by LPCVD, etch backside
   pattern, and etch front-side silicon nitride by RIE.

Substrate (Si)
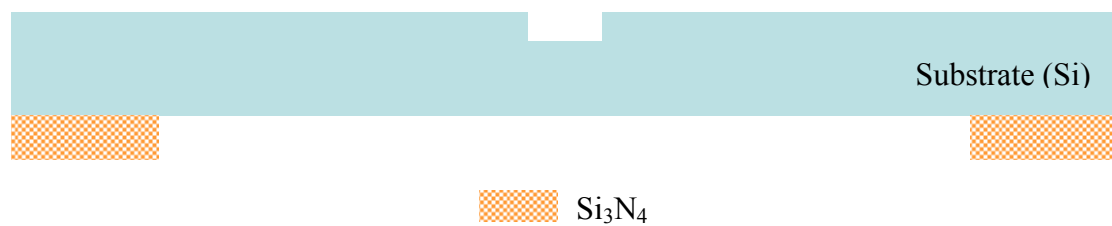
Si_3N_4

2. Etch silicon by RIE (to pattern microlens by mask 1).

Si₃N₄

3. Etch silicon by RIE (to pattern microlens by mask 2).

Si₃N₄   SU-8

4. Coat SU-8

Si₃N₄   SU-8

5. Etch backside silicon by KOH.

Figure 3-1: Fabrication process of binary mask.

Process flow:

In the first step, 1μm-thick Si_3N_4 was deposited on the RCA cleaned bare silicon wafer by LPCVD. Then on the Si_3N_4 backside layer was spin coated HMDS and a layer of photoresist FH6400 as the etching mask for the subsequent Si_3N_4 RIE. The same process was done again in the front-side. Next, the microlens were patterned and aligned to the mask 1 and 2 in the silicon layer. Then, KOH solution was used to etch the backside silicon to form the total structure.

3-2 Film mask process

The photoresist was characterized by using a film mask made of photographic films. The test pattern on the film mask is shown in Figure 3-2. In the first step, the transmittance of each square is measured by a laser beam and an optical power meter. Then the resist is exposed through the mask. The test process is simple, such as RCA clean, coating HMDS, spin-coating photoresist, soft bake, exposure, and development. Finally the depth of the developed photoresist is measured by WKYO. In Figure 3-3, the roughness is poor (Ra=37nm) such that the film mask will not be considered in device fabrication. Then the step height is transferred to etch depth and solubility. The relation to the transmittance and the solubility is shown in Figure 3-4. The solubility is the etch depth divided by the development time.

In Figure 3-4, there is a transition region of solubility for the transmittance value between 0.03 to 0.2. This transition range will be used in the gray-scale technology on the positive photoresist, AZ4620.
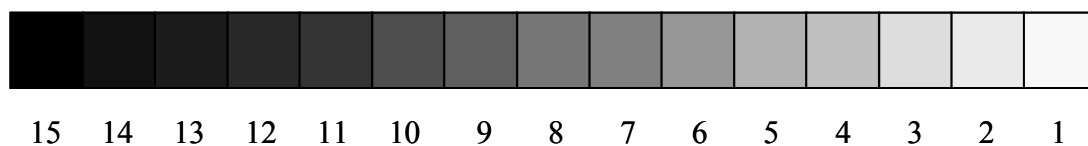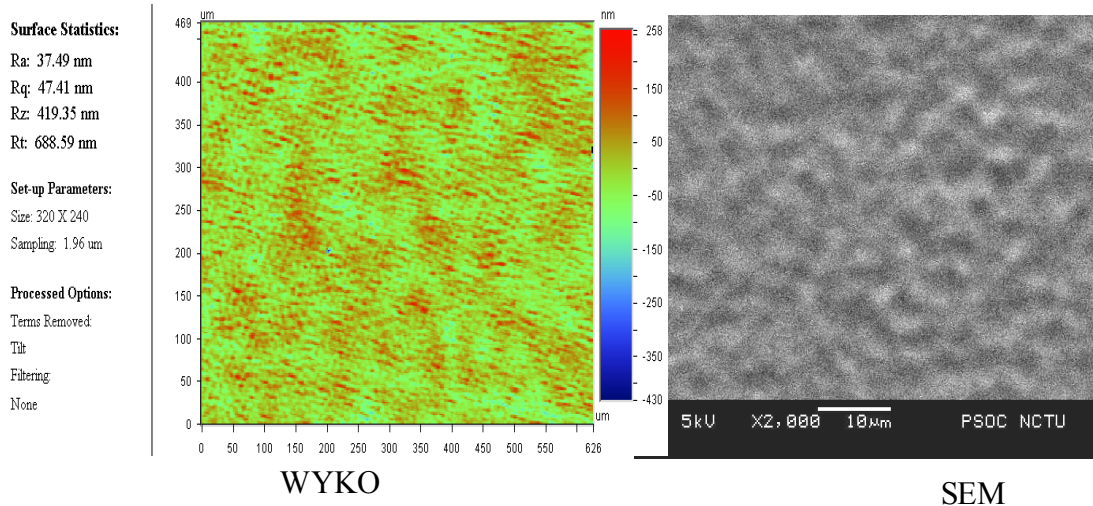

| 15 | 14 | 13 | 12 | 11 | 10 | 9 | 8 | 7 | 6 | 5 | 4 | 3 | 2 | 1 |

Figure 3-2: Schematic of the film test mask.

Surface Statistics:
Ra: 37.49 nm
Rq: 47.41 nm
Rz: 419.35 nm
Rt: 688.59 nm

Set-up Parameters:
Size: 320 X 240
Sampling: 1.96 um

Processed Options:
Terms Removed:
Tilt
Filtering:
None

WYKO   SEM

Ra=37nm Rz=491nm

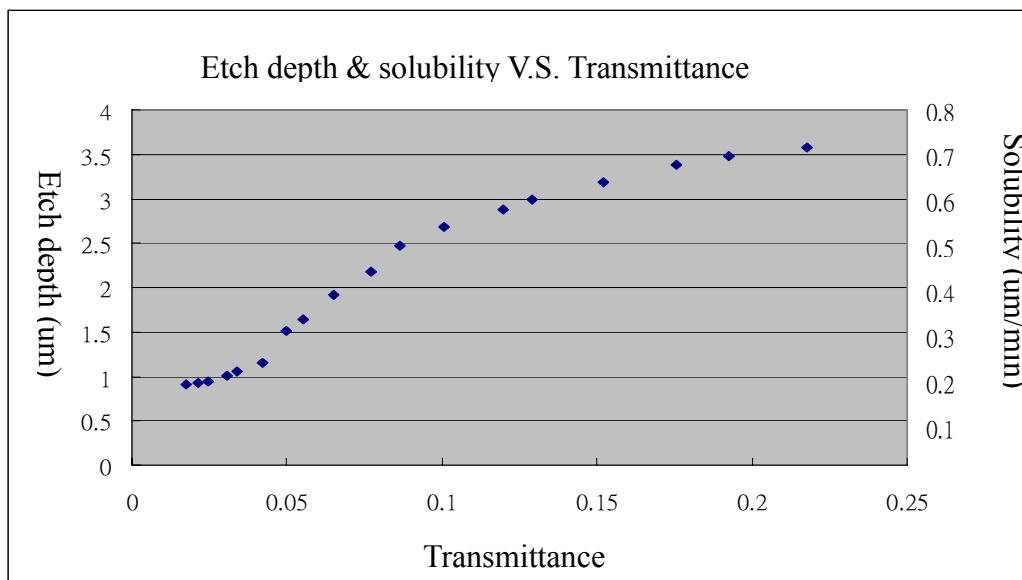Figure 3-3: Roughness of the test pattern with test mask.
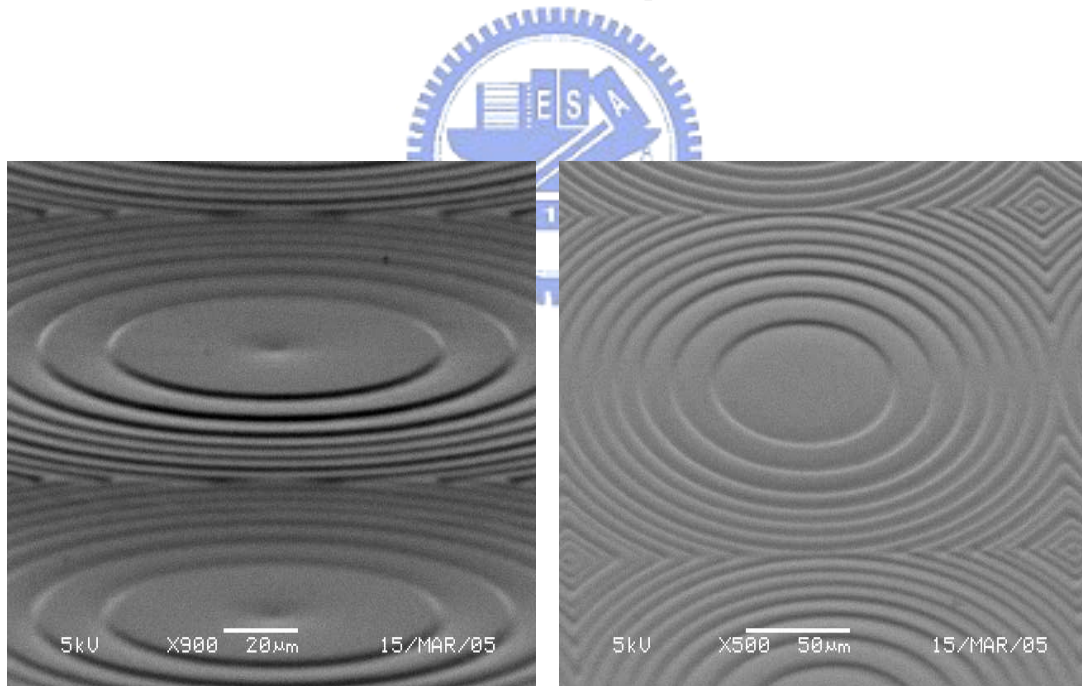

Figure 3-4: Relation of etch depth to transmittance of the film mask.
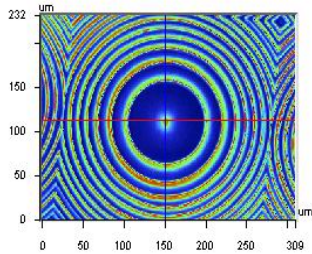
3-3 HEBS mask process

This section is about the test of a High Energy Beam Sensitive (HEBS) mask from Dr. 黃榮山 at National Taiwan University. This experiment is very simple. In the first step, the positive photoresist, AZ4620, is coated on a RCA cleaned bare silicon wafer. Then the microlens is patterned with the HEBS mask. After the

photoresist is developed, the experiment result is measured by different instrument, WYKO, SEM, and ET-4000 surface profilometer, as shown in Figure 3-5.

In Figure 3-5 (a), the profile measurement of the two different type microlenses by SEM are good. In Figure 3-5 (b), (c), and (d) all the measurements are right side in Figure 3-5 (a). Figure 3-5 (b) shows the profile measurement by WYKO Interferometer. Figure 3-5 (c) shows the profile measurement by ET-4000 surface profilometer. The middle circle thickness is 0.75μm. Figure 3-5 (d) shows the roughness of the photoresist (Ra=8.73), which is much better than the one with the film mask. So the HEBS mask can be a good way for gray-scale technology. However, In Figure 3-5 (c), the profile is better than in (b). The reason should be the interference effect which will be discussed in Chapter 4.
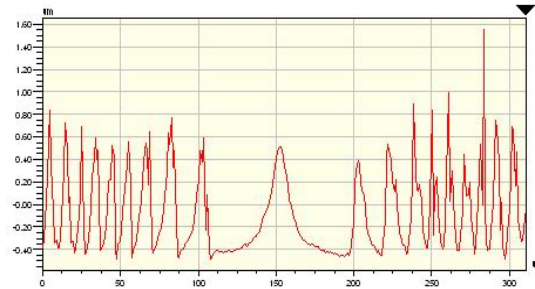

(a)

Veeco

X Profile

Rq	0.36 um
Ra	0.30 um
Rt	2.03 um
Rp	1.55 um
Rv	-0.48 um

Angle	1.09 mrad
Curve	46.33 mm
Terms	None
Avg Ht	-0.08 um
Area	-25.23 um2

Y Profile
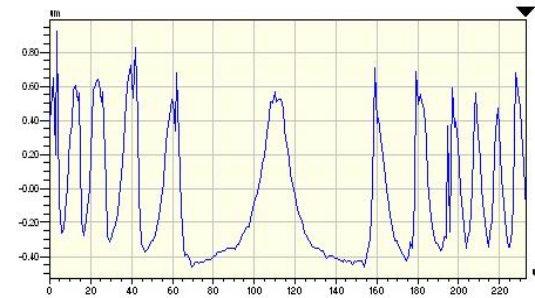
Rq	0.37 um
Ra	0.32 um
Rt	1.38 um
Rp	0.92 um
Rv	-0.46 um

Angle	-2.24 mrad
Curve	15.78 mm
Terms	None
Avg Ht	-0.04 um
Area	-8.60 um2

X	150.38	-	-	um
Y	113.52	-	-	um
Ht	0.47	-	-	um
Dist		-	-	um
Angle		-	-	°

Title:

(b)

P.profile |———————| 0.02mm Diff1:0.050um 2:0.746um 3:0.748um

V.mag.10000(5) H.mag.500(1)

(c)   Thickness=0.75 μm

38

Surface Statistics:
Ra: 290.45 nm
Rq: 339.23 nm
Rz: 2.62 um
Rt: 2.89 um

Set-up Parameters:
Size: 320 X 240
Sampling: 970.22 nm

Processed Options:
Terms Removed:
Curvature & Tilt
Filtering:
None

Ra = 8.73 nm

Surface Statistics:
Ra: 8.73 nm
Rq: 11.44 nm
Rz: 70.89 nm
Rt: 138.60 nm

Set-up Parameters:
Size: 55 X 45
Sampling: 970.22 nm

Processed Options:
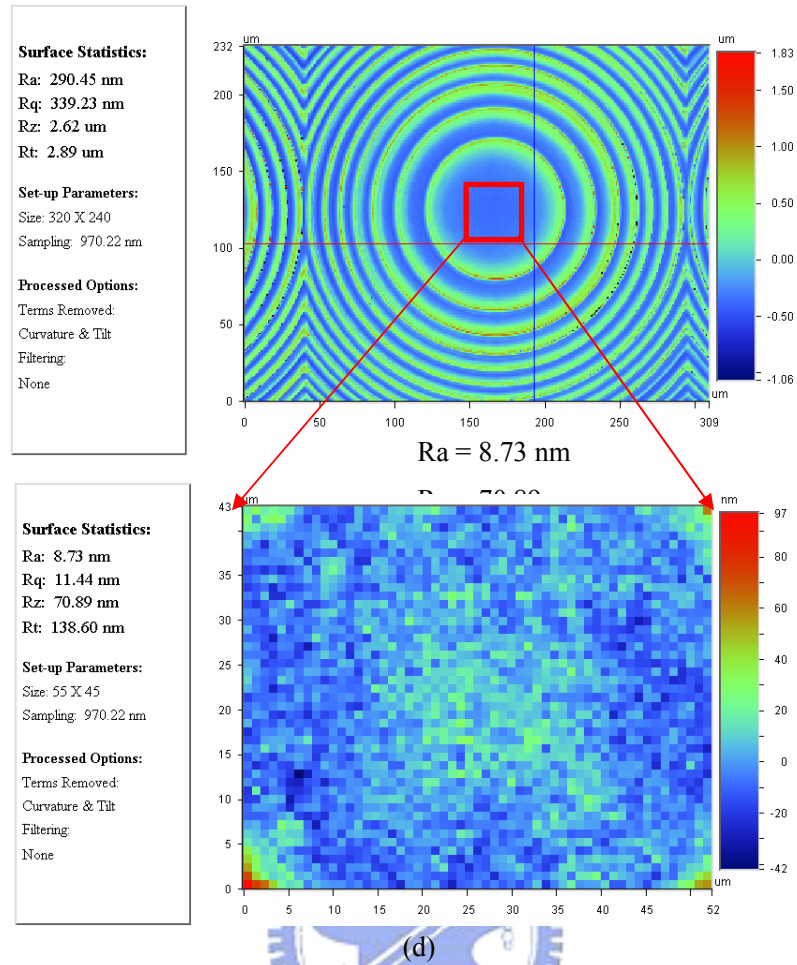Terms Removed:
Curvature & Tilt
Filtering:
None

(d)

Figure 3-5: (a) Profile measurement by SEM, (b) profile measurement by WYKO Interferometer, (c) profile measurement by ET-4000, and (d) roughness by WYKO.
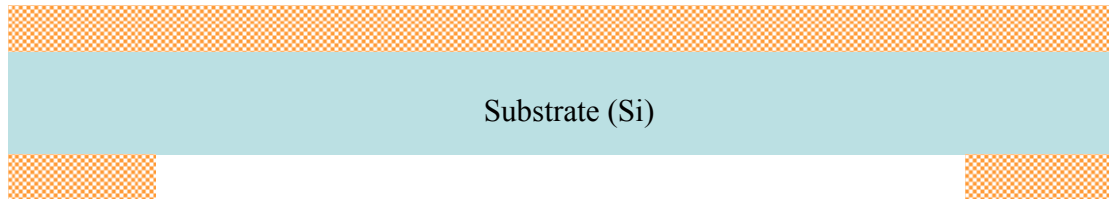
3-4 FIB mask and microlens fabrication process

The designed pattern is described in Chapter 2. The mask and microlens fabrication process are the same as follows. In the first step, 1μm-thick Si_3N_4 is deposited on the RCA cleaned bare silicon wafer by LPCVD. Then on the Si_3N_4 backside layer is spin coated HMDS and a layer of photoresist FH6400 as the etching mask for the subsequent Si_3N_4 RIE. Next, KOH solution is used to etch the backside silicon. Finally the FIB system is used to define the pattern on the Si_3N_4 layer.

Si₃N₄ ... Si$_3$N$_4$
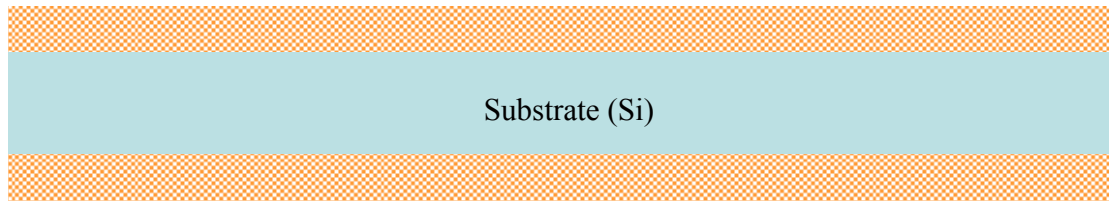
1. Deposit silicon nitride by LPCVD.

Substrate (Si)

Si$_3$N$_4$

2. Etch backside silicon nitride by RIE.

Substrate (Si)

Si$_3$N$_4$

3. Etch backside silicon by KOH.

Substrate (Si)

Si$_3$N$_4$

4. Define pattern by FIB

Figure 3-6: Fabrication process of FIB mask and the microlens.